NANO LETTERS

2007
Vol. 7, No. 10
3086−3091

Functionalized Carbon Nanotubes for Detecting Viral Proteins

Yian-Biao Zhang,[†,§] Mandakini Kanungo,[‡,§] Alexander J. Ho,[‡,||] Paul Freimuth,[†] Daniel van der Lelie,[*,†] Michelle Chen,[⊗] Samuel M. Khamis,[⊥] Sujit S. Datta,[⊥] A. T. Charlie Johnson,[*,⊥] James A. Misewich,[*,‡] and Stanislaus S. Wong[*,‡,#]

Biology Department, Brookhaven National Laboratory, Building 463, Upton, New York 11973, Condensed Matter Physics and Materials Science Department, Brookhaven National Laboratory, Building 480, Upton, New York 11973, Biomedical Engineering Department, State University of New York at Stony Brook, Stony Brook, New York 11794, Department of Materials Science and Engineering, University of Pennsylvania, Philadelphia, Pennsylvania 19104, Department of Physics and Astronomy, University of Pennsylvania, Philadelphia, Pennsylvania 19104, and Department of Chemistry, State University of New York at Stony Brook, Stony Brook, New York 11794

Received July 1, 2007; Revised Manuscript Received August 26, 2007

ABSTRACT

We investigated the biocompatibility, specificity, and activity of a ligand−receptor-protein system covalently bound to oxidized single-walled carbon nanotubes (SWNTs) as a model proof-of-concept for employing such SWNTs as biosensors. SWNTs were functionalized under ambient conditions with either the Knob protein domain from adenovirus serotype 12 (Ad 12 Knob) or its human cellular receptor, the CAR protein, via diimide-activated amidation. We confirmed the biological activity of Knob protein immobilized on the nanotube surfaces by using its labeled conjugate antibody and evaluated the activity and specificity of bound CAR on SWNTs, first, in the presence of fluorescently labeled Knob, which interacts specifically with CAR, and second, with a negative control protein, YieF, which is not recognized by biologically active CAR proteins. In addition, current−gate voltage (I–V_g) measurements on a dozen nanotube devices explored the effect of protein binding on the intrinsic electronic properties of the SWNTs, and also demonstrated the devices' high sensitivity in detecting protein activity. All data showed that both Knob and CAR immobilized on SWNT surfaces fully retained their biological activities, suggesting that SWNT−CAR complexes can serve as biosensors for detecting environmental adenoviruses.

In recent years, there has been growing interest in forming viable strategies for the controlled functionalization of single-walled nanotubes (SWNTs) with biological systems.[1−3] Such bio−nano integrated systems, combining the conducting and semiconducting properties of carbon nanotubes with the recognitive and catalytic properties of biomaterials, offer particular promise for developing novel biosensor systems. Specific recognition of target molecules is the essential feature for biological sensing. Accordingly, we have been interested in addressing the following key issues:

1. Do ligand−receptor proteins, bound onto SWNTs, retain their active configuration and conformation so as to remain amenable to biological interactions? We answered this question by demonstrating that functionally active Knob and CAR can be bound onto SWNT surfaces through an amide linkage generated via a diimide reagent.

2. Can this system subsequently be utilized for biological sensing? Our electrical measurements herein demonstrated the applicability of single biofunctionalized carbon nanotubes as field effect transistor (FET) biosensors wherein the biological moiety maintains its activity, proper binding conformation, and biospecificity.

Several different biomolecular systems have been previously affixed to the external surfaces of SWNTs with the goal of creating functional devices. For example, enzyme-coated SWNTs were used as sensors that either modulate their optical properties upon adsorption or alter their conductance upon variations in pH.[4,5] Viruses were employed to assemble SWNTs and other materials into organized networks.[6] Proteins such as ferritin, avidin, bovine serum albumin (BSA), and streptavidin,[7−9] as well as metallopro-

* To whom correspondence should be addressed. E-mail: vdlelied@bnl.gov (D.v.d.L.); cjohnson@physics.upenn.edu (A.T.C.J.); misewich@bnl.gov (J.A.M.); sswong@notes.cc.sunysb.edu (S.S.W.).

† Biology Department, Brookhaven National Laboratory.

‡ Condensed Matter Physics and Materials Science Department, Brookhaven National Laboratory.

§ These authors contributed equally to this work.

|| Biomedical Engineering Department, State University of New York at Stony Brook.

⊗ Department of Materials Science and Engineering, University of Pennsylvania.

⊥ Department of Physics and Astronomy, University of Pennsylvania.

Department of Chemistry, State University of New York at Stony Brook.

10.1021/nl071572l CCC: $37.00
Published on Web 09/26/2007

teins and enzymes[10] have been noncovalently bound onto SWNT surfaces so as to generate highly specific electronic biosensors. Other groups have coated peptides[11] with selective affinity for SWNTs onto their surfaces while different laboratories have bound proteins[12,13] such as either ferritin or BSA onto oxidized SWNTs via an amide linkage in aqueous solution. In these latter studies, the biological activities of the attached moieties were confirmed but the electrical activity of the functionalized nanotubes was not measured.

Although this is a relatively unexplored area of research, what is abundantly evident is that the covalent functionalization of biologically active ligand−receptor proteins onto single SWNTs and SWNT bundles clearly affords a viable strategy toward developing specific, quantitative biosensors. Precedence for such a strategy lies in a few unrelated studies. For instance, complementary detection of prostate-specific antigen was demonstrated by using In_2O_3 nanowire and SWNT devices.[14] SWNT-FET-based biosensors composed of either DNA aptamers[15] or single-stranded DNA[16] as molecular recognition elements were also reported, although most of this DNA work relied on noncovalent interactions with the SWNTs.

In the present study, we demonstrate a simple, fast-response, highly sensitive, real-time biosensor composed of a ligand−receptor protein complex covalently attached by a diimide linker to oxidized SWNTs via a mild, ambient, straightforward, and economical protocol. That is, we not only retained the intrinsic biological activity and specificity of the attached complex but also conserved the highly favorable electronic properties of SWNTs in these biofunctionalized single-tube devices. The proteins we used were the adenovirus protein, Ad12 Knob, and its complementary human "Coxsackie virus and adenovirus receptor", CAR.

Adenoviruses are one of many subclasses of viruses that cause infections such as the common cold and mild ailments of the upper respiratory and gastrointestinal tracts. Unlike viruses such as HIV, Ebola, and poliovirus, adenoviruses do not use either envelope proteins or capsid domains to infect cells. Rather, infection is initiated by the formation of a high affinity complex between the Knob trimer and its complementary adenovirus CAR receptor present in human cells. Upon binding CAR, the Knob-coated virus replicates within the cell nucleus, triggering infections.[17,18] Currently, adenoviruses are the leading candidates as vectors for gene therapy.[19] In our work, we used 6 mg/mL of purified Knob and 2.5 mg/mL of CAR protein, as verified by using a BCA assay kit.

Raw HiPco (high-pressure carbon monoxide decomposition process) SWNT bundles as well as individual SWNTs (prepared on surfaces by in situ catalytic chemical vapor deposition) were purified and air oxidized by using a modification of the gasification−dissolution method described earlier by Chiang et al.[20] This process generates surface functionalities on the nanotubes, particularly carboxylic acids at their ends and sidewalls. Air-oxidized SWNTs were then suspended in a 50 mM phosphate buffer (pH 8) solution at a concentration of 1 mg/mL. Proteins were attached to the processed SWNTs via a two-step process of carbodiimide (EDAC)-mediated activation previously described.[14] We confirmed that the proteins had, indeed, bound to the SWNTs by atomic force microscopy (AFM) height analysis. Further experimental details, including protein labeling, are given in the Supporting Information (Figures S1−S3).

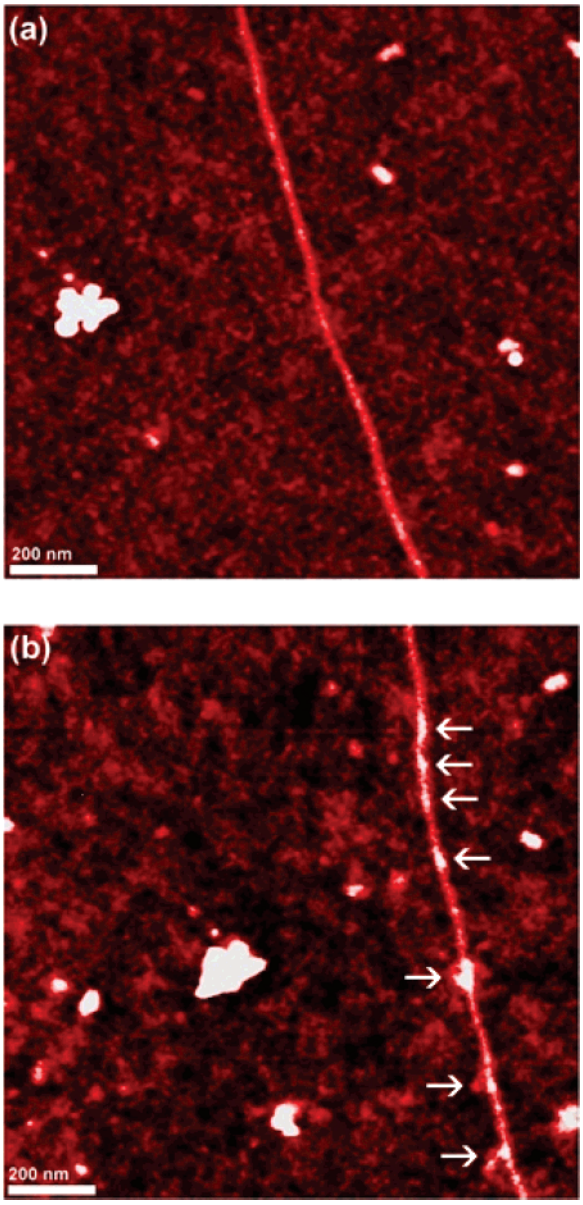

Figure 1. (a) AFM height image of single-walled carbon nanotubes on a Si/SiO_2 substrate after oxidation. The *z*-axis color scale is 10 nm. (b) AFM height image of the same nanotube after the attachment of the CAR protein and subsequent exposure to Knob protein. Arrows indicate seven main sites along the nanotube's length where the CAR + Knob complex is bound to the nanotube's surface. The vertical *z*-axis color scale is 10 nm. The images were low-pass filtered for clarity.

We obtained AFM measurements before and after protein attachment on four samples. Representative AFM height images and statistical analysis of selected cross sections (shown in Figure 1) conclusively showed that this functionalization procedure attaches protein complexes (CAR + Knob) along the length of the SWNT (on average, ~1 μm for individual tubes). The observed protein density in Figure 1 was approximately 1 per 200 nm, but in other samples, it approached the limit of the AFM resolution (~1 per 20 nm).

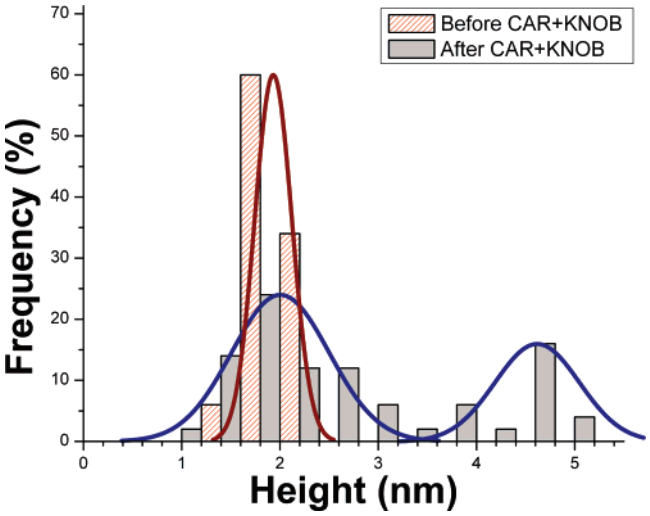

Figure 2. Histogram of SWNT diameters based on 50 equally spaced height sections from each AFM image with Gaussian fits. Before applying any proteins, the data (red, striped bars and red fit) show a SWNT diameter of 1.9 ± 0.2 nm. After applying CAR + Knob proteins, the distribution (gray bars and blue fits) exhibits *two* peaks, corresponding to heights of 2.0 ± 0.5 nm and 4.4 ± 4 nm, ascribed to regions of the nanotube without and with attached protein complexes, respectively.

Height analysis (Figure 2) demonstrated that the diameter of an individual SWNT bundle after oxidation was 1.9 ± 0.2 nm and that the additional height observed, associated with the attached protein complex (CAR + Knob), was 2.5 ± 0.2 nm. AFM measurements on five other samples exposed to CAR alone yielded a height increase of 0.5 nm (data not shown) so that by extension, the intrinsic height increase due to Knob itself was approximately 2 nm. These values are somewhat smaller than the accepted molecular sizes of these proteins, consistent with our expectation that (i) pressure from the AFM tip may have distorted the protein and that (ii) proteins attached to the mostly hydrophobic nanotube surface in air can be slightly different from their intrinsic morphology in aqueous solution. As demonstrated later and further corroborated in the Supporting Information (data on SWNT bundles, Figure S5), CAR proteins effectively attached to individual SWNTs as a single layer and retained their critical molecular recognition functionality.

After confirming the formation of our protein−SWNT constructs, we explored their interaction with both labeled complementary (Ad 12 Knob) and noncomplementary (YieF) proteins, thereby enabling us to assess the activity and specificity of the bound, attached proteins. Both Ad 12 Knob and YieF were labeled by using Alexa Fluor (Molecular Probes). All optical and fluorescence images of the labeled proteins were recorded by using a Zeiss Axiovert 200 fluorescence microscope.

The biological activity of bound Ad 12 Knob was investigated by targeting rhodamine-labeled anti-Knob antibodies to the oxidized SWNT−Knob constructs. These antibodies were purified by using an affinity column of immobilized Ad 12 Knob, and hence, we targeted only those Knob proteins folded in specifically active conformations. Nonspecific binding of rhodamine-labeled anti-Ad 12 Knob protein attached to carbon nanotubes was prevented by blocking this reaction with 4% milk, which contains a number of unrelated, nonspecific proteins in high concentrations. Figure 3a shows the optical image (left) and the corresponding fluorescence image (right) of fluorescently labeled anti-Knob antibodies targeting Ad 12 Knob protein bound to the carbon nanotubes. The fluorescence of the functionalized carbon nanotubes confirms that Ad 12 Knob bound to SWNTs indeed retains its biologically active conformation. As control experiments, labeled anti-Knob antibodies lacking protein were targeted to SWNTs either in the presence (blocked) or absence of milk (not blocked). In the latter case, we observed that the sample fluoresced, suggesting that the labeled antibodies bound to the SWNTs. Conversely, blocked SWNTs exhibited little or no fluorescence (Supporting Information Figure S4), demonstrating the efficacy of milk as a blocking agent. Hence, it is evident that labeled anti-Knob antibodies could specifically target bound Knob proteins on carbon nanotube surfaces.

By analogy, to investigate the biological activity and specificity of bound CAR, we used fluorescently labeled Knob, which shows high specific binding to CAR. In a separate control experiment, we attached YieF, an unrelated 22.4 kDa protein isolated from *E. coli* bacteria, to the SWNTs; YieF is nonspecific for CAR. Hence, the presence of bound CAR proteins in their biologically active conformation will show specificity to Knob proteins. SWNT−CAR constructs were blocked by 4% milk to prevent nonspecific binding of the labeled proteins to the nanotubes. Figure 3b shows an optical image (left) and the corresponding fluorescent image (right) of SWNT−CAR constructs targeted by fluorescently labeled Ad 12 Knob. The sample fluoresces, indicating that Knob is bound to the CAR proteins. On the other hand, after replacing the labeled Ad 12 Knob with labeled YieF, the samples did not fluoresce (Figure 3c). This observation afforded the following evidence: (1) CAR is bound to the carbon nanotubes, (2) bound CAR is biologically active, and (3) CAR-functionalized nanotubes will specifically bind to Ad 12 Knob. Thus, this construct provides us with the basis for a biological sensor to detect the presence of the Ad 12 Knob viral protein.

We measured current−gate voltage ($I-V_g$) data on a dozen nanotube devices to explore the effect of the attachment process and of protein binding on the SWNTs' electronic properties. Typical data are displayed in Figure 4. Nanotube FET devices were of high quality; they consisted of individual SWNTs with ON/OFF ratios exceeding 1000 and possessed on-state resistance values of 100−500 kΩ. Findings discussed below were reproduced in all the devices, although there was some scatter, as noted, in individual responses.

All devices showed a hysteretic $I-V_g$ response, as is typical of nanotube FETs on untreated silica substrates. This response results from charge injection from the nanotube into nearby regions due to the substantial electric field (~10 V/nm) existing at the SWNT surface associated with a large gate voltage (V_g).[21,22] The electric field of this injected

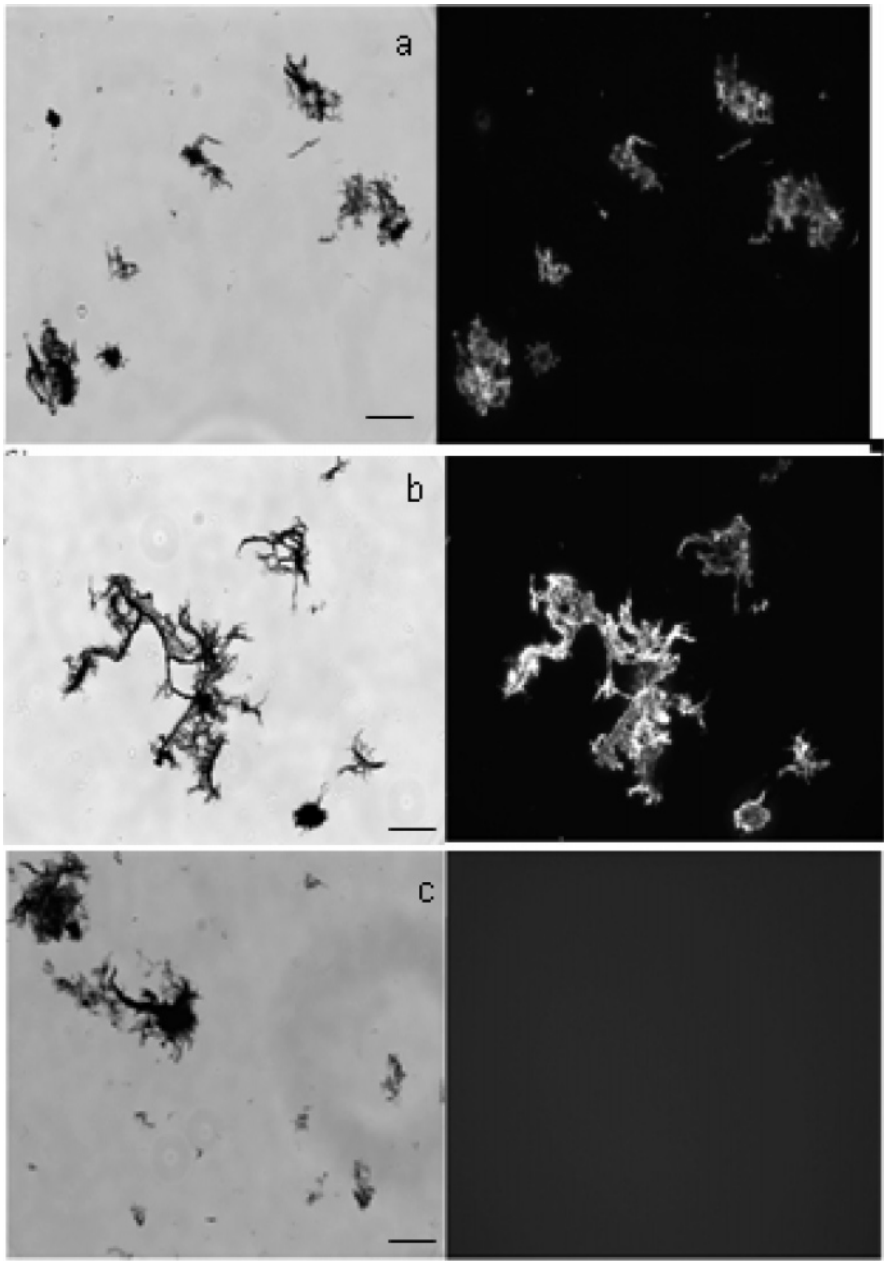

Figure 3. (a) Optical (left) and corresponding fluorescence (right) images of rhodamine-labeled anti-Knob antibodies targeting Ad12 Knob functionalized air-oxidized SWNTs. (b) and (c) show, respectively, the optical and corresponding fluorescence images of fluorescently labeled Ad 12 Knob and YieF targeting CAR-functionalized air-oxidized SWNTs. The sample in (b) fluoresces because the Ad 12 Knob is bound to CAR. On the other hand, there is no observable fluorescence in the sample in (c), where labeled YieF targets functionalized CAR air-oxidized SWNTs. All samples were blocked with milk to prevent the nonspecific binding of proteins onto the SWNT surfaces. The scale bar is 2.5 μm.

charge and of other charge traps near the SWNT is partially screened when the FET is in its ON state, while almost no screening occurs when the FET is in the OFF state. Hence, in the following discussion, we assume that the leftmost (ON-to-OFF) transition of the $I-V_g$ characteristic is more reproducible than the OFF-to-ON transition in the presence of unavoidable charge switching and is, therefore, more amenable to physical interpretation.

The oxidation process typically either increased the ON state current of the device (by 10−25%) or left it unchanged (Figure 4). We concluded that mild oxidation created a low density of defect sites that did not degrade electron transport in the device; we attribute the small increase in the ON state current to contact annealing. Oxidation also generated a reproducible increase of 0.5−3 V in the ON−OFF threshold voltage, consistent with the notion that defect sites created by oxidation are functionalized with oxygenated moieties (such as predominantly carboxyl groups) that become deprotonated in the presence of adsorbed water. This change leaves the groups negatively charged, so that a more positive value of V_g is needed to turn the FET OFF. Assuming a typical backgate capacitance of 25 aF/μm for this geometry, this shift in V_g corresponds to an increase in the carrier density of 80−400 holes/μm.

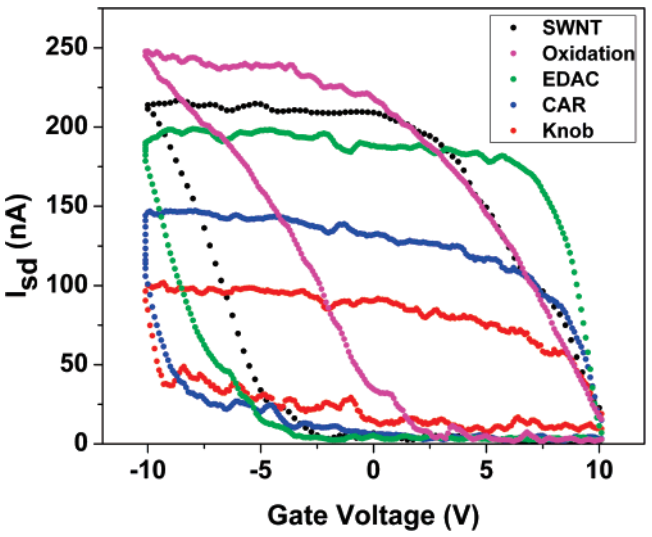

Figure 4. Measured source−drain current as a function of gate voltage for a SWNT FET demonstrates that covalently bound CAR protein retains its molecular recognition functionality. Data are shown for as-grown SWNT (black), SWNTs after oxidation (purple), after exposure to EDAC/NHS (green), upon CAR attachment (blue), and after exposure to the complementary Knob protein (red). The data indicate that Knob specifically binds to the CAR, leading to a significant decrease (~33%) in the ON-state current of the FET. The bias voltage is 100 mV for all measurements.

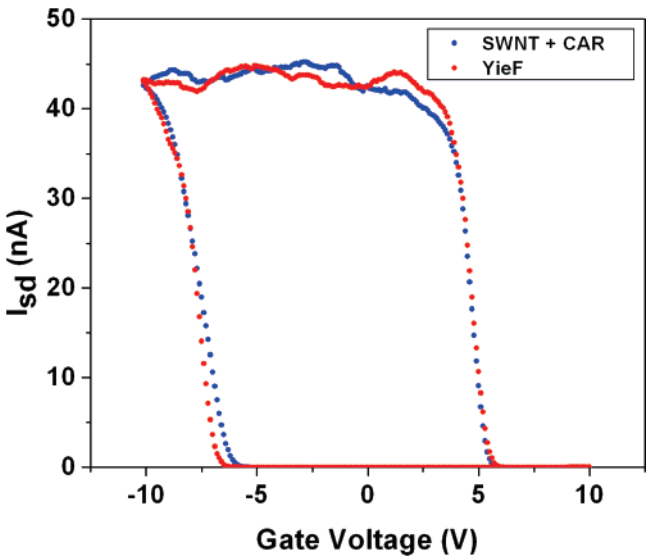

Figure 5. Measured source−drain current vs gate voltage for a SWNT sensor functionalized with CAR protein (blue data) shows no response when exposed to the nonspecific YieF protein (red).

Subsequently, incubating the device in EDAC/NHS solution engendered a negative shift of the threshold voltage to its original value or to an even more negative voltage, in agreement with the expectation that the proton had been replaced by a stable active ester.[12] CAR protein attachment led to a 1−2 V decrease in the ON−OFF threshold voltage and a corresponding 20−40% decrease in the ON-state current. These observations are consistent with the FET experiencing a positive charge and enhanced carrier scattering due to the presence of the protein, as other groups have proposed.[7,23,24] Finally, exposing the CAR−SWNT hybrid to the complementary Knob protein further suppresses the ON state current; the molecular recognition event was thus fully detectable in this system (Figure 4). To quantify the extent of protein binding, we can reasonably assume that the nanotube is 1 μm long, with a corresponding protein density of 1 per 20 nm. Hence, on average, 50 proteins coat the nanotube and the corresponding decrease in current we observed is approximately 1 nA/protein, a sizable value enabling the detection of single protein molecules. Because the applied voltage is 100 mV, the resistance of CAR and of Knob bound to CAR is approximately 667 kΩ and 1 MΩ, respectively, implying a resistance of about 5 kΩ/protein. Using the Landauer formulation in the incoherent transport regime, we thereby obtain a reflection coefficient of approximately 40% per protein, implying that the protein complex is closely bound to the nanotube surface.

In a separate control experiment (Figure 5), CAR-functionalized devices showed no evident change in $I-V_g$ response, as expected, after exposure to (noncomplementary) YieF, implying that the in vivo chemical specificity of the CAR protein is retained even when it is immobilized on the SWNT surface. In another experiment, we noted that the electrical profile of SWNTs, which had been noncovalently functionalized with CAR proteins, reverted to its original signal upon extended washing with phosphate buffer and water; these data highlighted the importance of covalent protein binding in our experiments and implied that weakly bound, physically absorbed proteins were lost upon washing of the SWNTs (data not shown).

The present study provides proof-of-concept for developing a simple, efficient, sensitive, fast-response, and real-time miniaturized nanotube FET biosensor for detecting the Ad 12 Knob virus using CAR−Knob specificity. Moreover, this methodology can be extended to uncover the presence of serotype12 and all other possible CAR-binding adenoviruses (about 30 serotypes, including Ad2 and Ad5), as well as subgroup B Coxsackie viruses. This is the first evidence of straightforward, ambient covalent immobilization of a viral ligand−receptor-protein system onto individual SWNTs and SWNT bundles and of our subsequent confirmation of the bound proteins' retention of biological activity and specificity, as revealed by systematic electrical measurements. Our future goal will be to develop a single-molecule biosensor based on the conductivity change of a single SWNT by adding a discrete CAR domain to the nanotube.

Acknowledgment. Y.Z., D.v.d.L., J.M., and S.S.W. acknowledge support of this work through the U.S. Department of Energy Office of Basic Energy Sciences under contract DE-AC02-98CH10886. S.S.W. also thanks the National Science Foundation (CAREER DMR-0348239) as well as the Alfred P. Sloan Foundation for supplies and financial support. Work conducted in the laboratory of A.T.C.J. was supported by the JSTO DTRA as well as the Army Research Office grant no. W911NF-06-1-0462; research at UPenn was also partially supported by the Nano/Bio Interface Center through the National Science Foundation under contract NSEC DMR-0425780. We thank A. Woodhead for helpful comments.

Supporting Information Available: Expression and purification of AD 12 Knob; CAR protein purification; YieF purification; fluorescent labeling of proteins; preparation of SWNT−protein hybrids; microscopy characterization of SWNTs and of SWNT−protein hybrids; attachment of labeled proteins onto SWNT−protein hybrids; growth, fabrication, and electrical measurements of SWNTs; additional AFM height measurements on SWNT bundles.

References

(1) Katz, E.; Willner, I. *ChemPhysChem* **2004**, *5*, 1084−1104.
(2) Bianco, A.; Prato, M. *Adv. Mater.* **2003**, *15*, 1765−1768.
(3) Wong, S. S.; Joselevich, E.; Woolley, A. T.; Cheung, C. L.; Lieber, C. M. *Nature* **1998**, *394*, 52−55.
(4) Baron, P. W.; Baik, S.; Heller, D. A.; Strano, M. S. *Nat. Mater.* **2005**, *4*, 86−92.
(5) Besteman, K.; Lee, J.-O.; Wiertz, F. G. M.; Heering, H. A.; Dekker, C. *Nano Lett.* **2003**, *3*, 727−730.
(6) Portney, N. G.; Singh, K.; Chaudhary, S.; Destito, G.; Schneemann, A.; Manchester, M.; Ozkan, M. *Langmuir* **2005**, *21*, 2098−2103.
(7) Chen, R. J.; Bangsarnutip, S.; Drouvalakis, K. A.; Kam, N. W. S.; Shim, M.; Kim, W.; Utz, P. J.; Dai, H. *Proc. Natl. Acad. Sci. U.S.A.* **2003**, *100*, 4984−4989.
(8) Shim, M.; Kam, N. W. S.; Chen, R. J.; Li, Y.; Dai, H. *Nano Lett.* **2002**, *2*, 285−288.
(9) Chen, R. J.; Zhang, Y.; Wang, D.; Dai, H. *J. Am. Chem. Soc.* **2001**, *123*, 3838−3839.
(10) Azamian, B. R.; Davis, J. J.; Coleman, K. S.; Bagshaw, C. B.; Green, M. L. H. *J. Am. Chem. Soc.* **2002**, *124*, 12664−12665.
(11) Wang, S.; Humphreys, E. S.; Chung, S.-Y.; Delduco, D. F.; Lustig, S. R.; Wang, H.; Parker, K. N.; Rizzo, N. W.; Subramoney, S.; Chiang, Y.-M.; Jagota, A. *Nat. Mater.* **2003**, *2*, 196−200.
(12) Jiang, K.; Schadler, L. S.; Seigel, R. W.; Zhang, X.; Zhang, H.; Terrones, M. *J. Mater. Chem.* **2004**, *14*, 37−39.
(13) Huang, W.; Taylor, S.; Fu, K.; Lin, Y.; Zhang, D.; Hanks, T. W.; Rao, A. M.; Sun, Y.-P. *Nano Lett.* **2002**, *2*, 311−314.
(14) Li, C.; Curreli, M.; Lin, H.; Lei, B.; Ishikawa, F. N.; Datar, R.; Cote, R. J.; Thomson, M. E.; Zhou, C. *J. Am. Chem. Soc.* **2005**, *127*, 12484−12485.
(15) So, H.-M.; Won, K.; Kim, Y. H.; Ryu, B. H.; Na, P. S.; Kim, H.; Lee, J.-O. *J. Am. Chem. Soc.* **2005**, *127*, 11906−11907.
(16) Staii, C.; Johnson, A. T., Jr.; Chen, M.; Gelperin, A. *Nano Lett.* **2005**, *5*, 1774−1778.
(17) Freimuth, P.; Springer, K.; Berard, C.; Hainfeld, J.; Bewley, M.; Flanagan, J. M. *J. Virol.* **1999**, *73*, 1392−1398.
(18) Bewley, M. C.; Springer, K.; Zhang, Y.-B.; Freimuth, P.; Flanagan, J. M. *Science* **1999**, *286*, 1579−1583.
(19) Nabel, G. J. *Proc. Natl. Acad. Sci. U.S.A.* **1999**, *96*, 324−326.
(20) Chiang, I. W.; Brinson, B. E.; Huang, A. Y.; Willis, P. A.; Bronikowski, M. J.; Margrave, J. L.; Smalley, R. E.; Hauge, R. H. *J. Phys. Chem. B* **2001**, *105*, 8297−8301.
(21) Radosavljevic, M.; Freitag, M.; Thadani, K. V.; Johnson, A. T. *Nano Lett.* **2002**, *2*, 761−764.
(22) Führer, M. S.; Kim, B. M.; Durkop, T.; Brintlinger, T. *Nano Lett.* **2002**, *2*, 755−759.
(23) Chen, R. J.; Choi, H. C.; Bansaruntip, S.; Yenilmez, E.; Tang, X. W.; Wang, Q.; Chang, Y. L.; Dai, H. *J. Am. Chem. Soc.* **2004**, *126*, 1563−1568.
(24) Star, A.; Gabriel, J. C. P.; Bradley, K.; Grüner, G. *Nano Lett.* **2003**, *3*, 459−463.

NL071572L